

# Composition design and mechanical properties of mixed (Ce,Y)-TZP ceramics obtained from coated starting powders

S.G. Huang<sup>a</sup>, J. Vleugels<sup>a,\*</sup>, L. Li<sup>b</sup>, O. Van der Biest<sup>a</sup>, P.L. Wang<sup>c</sup>

<sup>a</sup> Department of Metallurgy and Materials Engineering, Katholieke Universiteit Leuven, B-3001 Leuven, Belgium

<sup>b</sup> School of Material Science and Engineering, Shanghai University, Shanghai 200072, China

<sup>c</sup> State Key Lab of High Performance Ceramics and Superfine Microstructure, Shanghai Institute of Ceramics, Chinese Academy of Sciences, Shanghai 200050, China

Received 10 April 2004; received in revised form 1 July 2004; accepted 10 July 2004

Available online 1 September 2004

## Abstract

The microstructure and mechanical properties of a selection of ceramics with compositions in the low ceria and yttria corner of the  $ZrO_2$ – $CeO_2$ – $Y_2O_3$  system were investigated and evaluated. The calculated isothermal section of the  $ZrO_2$ – $CeO_2$ – $Y_2O_3$  system at 1450 °C was used to define the  $CeO_2$  content range of interest resulting in an optimum amount of tetragonal  $ZrO_2$  phase for TZP ceramics with an overall yttria content of 2 and 1 mol%. Pure monoclinic  $ZrO_2$  starting powder was coated with the appropriate amount of yttria and ceria stabiliser by means of a suspension coating technique and pressureless sintered in air at 1450 °C. The indentation toughness and Vickers hardness were evaluated as a function of the sintering time, grain-size and stabiliser content. An excellent fracture toughness of 13–15 MPa m<sup>1/2</sup> was obtained for  $ZrO_2$  ceramics with 1 mol%  $Y_2O_3$  + 4 mol%  $CeO_2$ , sintered for 1–4 h at 1450 °C.

© 2004 Elsevier Ltd. All rights reserved.

**Keywords:**  $ZrO_2$ ; Sintering; Microstructure; Mechanical properties; Thermodynamics; TZP; Coatings

## 1. Introduction

Tetragonal zirconia polycrystals (TZP) exhibit excellent mechanical properties such as strength and fracture toughness.<sup>1,2</sup> The high toughness is due to the stress-induced martensitic transformation from the tetragonal (t- $ZrO_2$ ) to the monoclinic (m- $ZrO_2$ ) zirconia phase. Yttria-doped zirconia with 2–3 mol%  $Y_2O_3$  exhibits a very high strength and fracture toughness. However, the mechanical properties of Y-TZP are greatly degraded by low temperature ageing at 200–300 °C in a humid atmosphere and hot aqueous solution.<sup>3,4</sup> The degradation is due to a spontaneous transformation from t- $ZrO_2$  to m- $ZrO_2$ , accompanied by the formation of micro-cracks during ageing. On the other hand,  $CeO_2$ -stabilized TZP ceramics have a considerably higher hy-

drothermal stability than Y-TZP under similar conditions.<sup>5,6</sup> In the  $ZrO_2$ – $CeO_2$  system, stabilization of t- $ZrO_2$  occurs over a wide composition range from 12 to 20 mol%  $CeO_2$ , with a preferred composition of 12 mol% ceria.<sup>6</sup> Moreover, experimental investigations revealed that the hydrothermal stability of Y-TZP can be significantly improved by doping with a suitable amount of ceria.<sup>7–9</sup> A homogeneous dispersion of fine  $Al_2O_3$  grains into a TZP matrix has been reported to suppress grain growth and increase the hardness, elastic modulus as well as the hydrothermal stability of the t- $ZrO_2$  phase.<sup>10</sup> Recently, it was found that the properties of Y-TZP/ $Al_2O_3$  and Ce-TZP/ $Al_2O_3$  composites obtained from yttria and ceria-coated zirconia powders are more attractive than those of co-precipitated powder based ceramics.<sup>11–13</sup>

In the present study, thermodynamic calculations were conducted to determine the stabiliser range in the  $ZrO_2$ – $CeO_2$ – $Y_2O_3$  system at 1450 °C. After selecting the proper compositions,  $CeO_2$  and  $Y_2O_3$  co-stabilised zirconia

\* Corresponding author. Tel.: +32 16 321244; fax: +32 16 321992.

E-mail address: [jozef.vleugels@mtm.kuleuven.ac.be](mailto:jozef.vleugels@mtm.kuleuven.ac.be) (J. Vleugels).

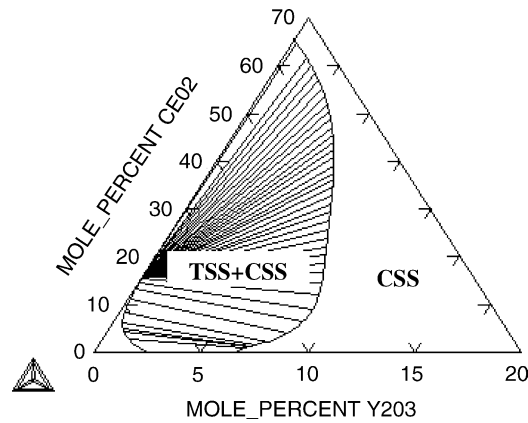


Fig. 1. Calculated partial phase diagram of the  $\text{ZrO}_2\text{--Y}_2\text{O}_3\text{--CeO}_2$  system at  $1450^\circ\text{C}$ .

powders were synthesized by a colloidal coating technique and pressureless sintered in air. The influence of the stabiliser content and composition on the microstructure, grain-size, fracture toughness and hardness of the ceramics are investigated and evaluated.

## 2. Composition selection

Although some experimental findings in the ternary  $\text{ZrO}_2\text{--CeO}_2\text{--Y}_2\text{O}_3$  system have been published,<sup>3,4,7–9</sup> no complete phase diagram of this system, especially on the relation between the tetragonal and cubic solid solution (Tss/Css) ratio and the overall composition has been reported. The isothermal section of the  $\text{ZrO}_2$ -rich corner of the  $\text{ZrO}_2\text{--CeO}_2\text{--Y}_2\text{O}_3$  system at  $1450^\circ\text{C}$ , extrapolated with the optimised thermodynamic data from Li et al.<sup>14,15</sup> using Thermo-Calc<sup>16</sup> is presented in Fig. 1. Fig. 2 shows the calculated Tss and Ccss phase relation for a 1 and 2 mol%  $\text{Y}_2\text{O}_3$  stabilised (Y,Ce)-TZP as a function of the  $\text{CeO}_2$  content up to 12 mol%. It is obvious that a lower stabiliser content corresponds to a higher Tss/Ccss ratio at  $1450^\circ\text{C}$ . For example, a (2Y,4Ce)-TZP contains 9.8 mol% Ccss, whereas only 0.4 mol% Ccss is calculated for a (2Y,2Ce)-TZP at  $1450^\circ\text{C}$ .

Table 1

Ceramic grades, composition, calculated Tss–Ccss phase content at  $1450^\circ\text{C}$ , calculated  $T_0$ , the temperature at which the chemical energy of the t- and m- $\text{ZrO}_2$  phase are equal, and the calculated martensitic transformation temperature,  $M_s$

Ceramic	CeO <sub>2</sub> (mol%)	Y <sub>2</sub> O <sub>3</sub> (mol%)	Al <sub>2</sub> O <sub>3</sub> (wt.%)	Tss (mol%)	Ccss (mol%)	$T_0$ (°C)	Grain-size <sup>a</sup> (μm)	$M_s$ (°C)
2Y2Al	0	2	2	100	0	519	1.55	–16
2Y1Ce2Al	1	2	2	100	0	508	1.37	–20
2Y2Ce2Al	2	2	2	99.6	0.4	486	1.39	–25
2Y4Ce2Al	4	2	2	90.2	9.8	426	1.10	–64
1Y2Ce2Al	2	1	2	100	0	688	1.54	36
1Y4Ce2Al	4	1	2	100	0	629	1.38	11
1Y6Ce2Al	6	1	2	100	0	538	1.97	–2
1Y8Ce2Al	8	1	2	96.6	3.4	438	1.62	–54

<sup>a</sup> The maximum measured grain-size intercept, used for the  $M_s$  calculation.

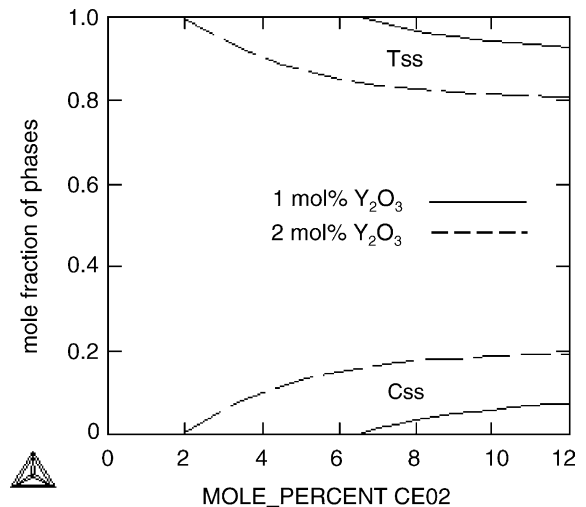


Fig. 2. Calculated Tss and Ccss phase content for 1 and 2 mol%  $\text{Y}_2\text{O}_3$  co-stabilised (Y,Ce)-TZP ceramics as a function of the  $\text{CeO}_2$  content at  $1450^\circ\text{C}$ .

Based on the calculated phase relations, the  $\text{CeO}_2$  stabiliser content for a 1 mol%  $\text{Y}_2\text{O}_3$  stabilised material was varied from 2 to 8 mol%, whereas the  $\text{CeO}_2$  content for a 2 mol%  $\text{Y}_2\text{O}_3$  stabilised grade was varied from 0 to 4 mol%, in order to investigate fully tetragonal ( $1450^\circ\text{C}$ ) as well as tetragonal ceramics with a small amount of cubic phase. The selected compositions and nomenclature of the different ceramic grades are summarized in Table 1.

## 3. Experimental procedure

Pure monoclinic  $\text{ZrO}_2$  nanopowder (Tosoh grade TZ-0) was coated with the appropriate amount of yttria and ceria by means of a suspension coating technique.<sup>11–13</sup> The chemicals used are  $\text{Y}_2\text{O}_3$  (grade YT-603, Atlantic equipment Engineers), cerium nitrate hexahydrate ( $\text{Ce}(\text{NO}_3)_3 \cdot 6\text{H}_2\text{O}$ , Aldrich Chemical Company) and ethanol.  $\text{Y}(\text{NO}_3)_3$  was prepared by the dissolution of  $\text{Y}_2\text{O}_3$  in  $\text{HNO}_3$  (65%).  $\text{Al}_2\text{O}_3$  (2 wt.%) powder (grade SM8, Baikowski,  $0.6\ \mu\text{m}$ ) was added to all powder mixture grades.

To break the agglomerates in the  $\text{ZrO}_2$  starting powder, Y-TZP milling balls (Tosoh grade TZ-3Y) with a diameter

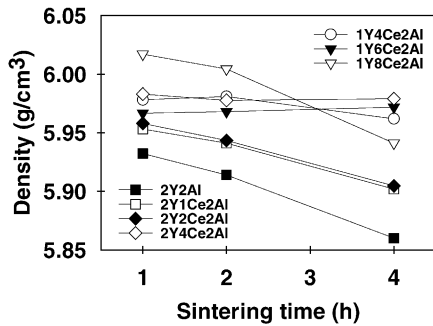


Fig. 3. Density of  $2Y_xCe_2Al$  and  $1Y_xCe_2Al$  ceramics as a function of  $CeO_2$  content and sintering time at  $1450^\circ C$ .

of 10 mm were added to the ethanol suspension containing cerium nitrate, yttrium nitrate and  $m-ZrO_2$  nanopowder. To avoid contamination, mixing was performed in polyethylene containers. After mixing for 36 h on a multi-directional mixer (type Turbula), water and ethanol were removed from the suspension by a rotating evaporator at  $95^\circ C$ . The dried powders were subsequently calcined in alumina crucibles in air at  $800^\circ C$  for 1 h. Due to the relative hard nature of the calcined powder agglomerates, a similar second mixing process was performed in ethanol to obtain soft agglomerates. The soft powder agglomerates were shaped in small cylinders ( $\varnothing$  and  $L = 10$  mm) by cold isostatic pressing (CIP) at 300 MPa for 3 min. Sintering was performed at  $1450^\circ C$  for 1–4 h in a tube furnace under a dry air flow of 100 ml/min at a heating rate of  $20^\circ C/min$  from 25 to  $1000^\circ C$  and  $10^\circ C/min$  from 1000 to  $1450^\circ C$ . Cooling was performed at  $20^\circ C/min$ .

The Archimedes technique was applied to measure the density (BP210S balance, Sartorius AG, Germany) of the samples in ethanol. Phase identification was carried out by X-ray diffraction (XRD, 3003-TT, Seifert, Ahrensburg, Germany) using  $Cu K\alpha$  radiation (40 kV, 30 mA). The XRD profiles were scanned in  $0.02^\circ$  step increments from  $20^\circ$  to  $40^\circ$  to determine the  $m-ZrO_2/(t+c)-ZrO_2$  ratio. The as-sintered samples were thermally etched in air at  $1350^\circ C$  for 30 min after polishing, and investigated by scanning electron microscopy (SEM, XL30-FEG, FEI, The Netherlands). The average grain-size was determined by IMAGE-PRO software according to the line intercept method<sup>17</sup> technique measuring about 1000 grains. The average grain-size data are presented as measured since no mathematical corrections were performed. The Vickers hardness  $HV_{30}$  was measured on a Zwick hardness tester with an indentation load of 30 kg. The indentation fracture toughness,  $K_{IC}$ , was obtained from the radial crack pattern of  $HV_{30}$  indentations, and the toughness was calculated according to the formula of Anstis et al.<sup>18</sup> using an elastic modulus of 200 GPa. The reported values are the mean and standard deviation of at least five indentations.

#### 4. Results and discussion

The density of the  $2Y_xCe_2Al$  and  $1Y_xCe_2Al$  ceramics sintered at  $1450^\circ C$  is presented as a function of the sintering

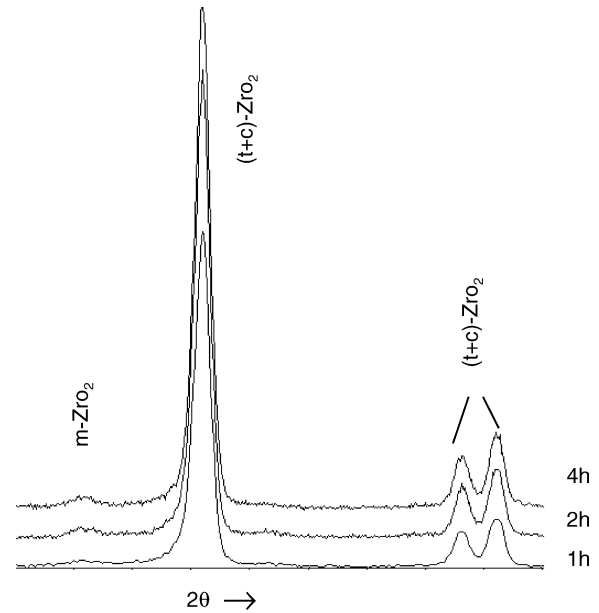


Fig. 4. XRD patterns for  $2Y_2Al$  sintered at  $1450^\circ C$  for 1–4 h.

time in Fig. 3, indicating that the density of most material grades gradually decreased with increasing sintering time. As revealed by XRD analysis on polished samples, the decreased density at longer sintering times should be attributed to the martensitic transformation of the  $t-ZrO_2$  phase and the concomitant formation of microcracks. The  $1Y_4Ce_2Al$ ,  $1Y_6Ce_2Al$  and  $2Y_4Ce_2Al$  grades, however, remain fully tetragonal even after sintering for 4 h at  $1450^\circ C$ . The appearance of a small amount of  $m-ZrO_2$  in the diffraction pattern after longer sintering times is illustrated for the  $2Y_2Al$

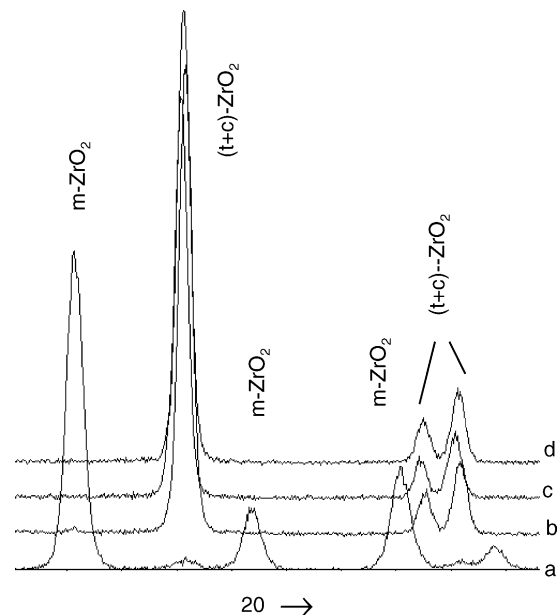


Fig. 5. XRD patterns of  $(1Y_xCe)-TZP$  sintered for 1 h at  $1450^\circ C$ , (a)  $1Y_2Ce_2Al$ , (b)  $1Y_4Ce_2Al$ , (c)  $1Y_6Ce_2Al$  and (d)  $1Y_8Ce_2Al$ .

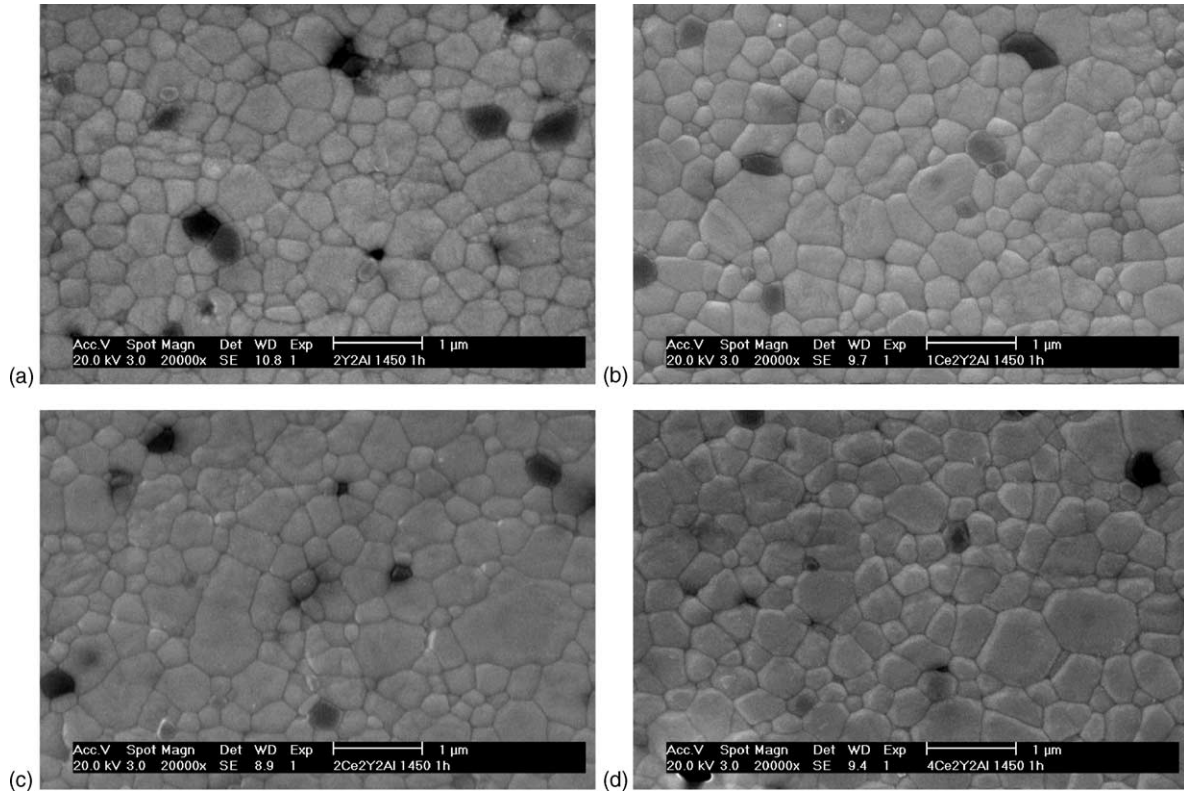


Fig. 6. SEM micrographs of thermally etched 2Y2Al (a), 2Y1Ce2Al (b), 2Y2Ce2Al (c) and 2Y4Ce2Al (d) ceramics sintered at 1450 °C for 1 h. The dark grains are Al<sub>2</sub>O<sub>3</sub> particles.

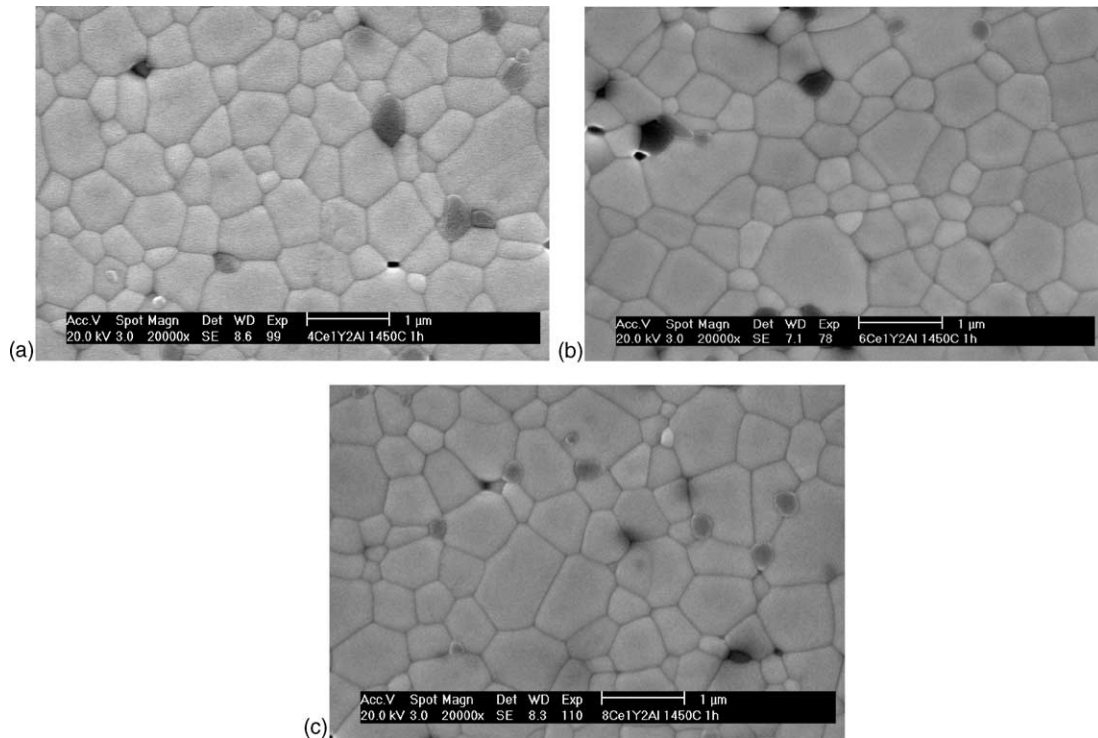


Fig. 7. SEM images for samples 1Y4Ce2Al (a), 1Y6Ce2Al (b) and 1Y8Ce2Al (c) sintered for 1 h at 1450 °C. The dark grains are Al<sub>2</sub>O<sub>3</sub> particles.

material grade in Fig. 4. All investigated material grades, except 1Y2Ce2Al, are fully tetragonal after sintering for 1 h at 1450 °C, as presented in Fig. 5. It is obvious that the amount of stabilizer in the 1Y2Ce2Al ceramic is not enough to stabilize the t-ZrO<sub>2</sub> phase during cooling. However, the addition of more CeO<sub>2</sub>, such as 4 mol% CeO<sub>2</sub> to a 1 mol% Y<sub>2</sub>O<sub>3</sub> is sufficient to retain t-ZrO<sub>2</sub> at room temperature. Y<sub>2</sub>O<sub>3</sub> (1 mol%) has never been reported to be enough to stabilize the tetragonal phase in a Y-TZP at room temperature.<sup>20</sup> It should, however, be mentioned that it is almost impossible to differentiate the T<sub>ss</sub> and C<sub>ss</sub> phase by means of XRD, implying that the fully tetragonal samples might contain a minor amount of c-ZrO<sub>2</sub>.

SEM micrographs of the thermally etched 2Y<sub>x</sub>Ce2Al and 1Y<sub>x</sub>Ce2Al material grades sintered for 1 h at 1450 °C are presented in Figs. 6 and 7. The dispersed alumina crystals, dark on the backscattered electron images, are pinned at the junctions of zirconia boundaries. The main microstructural difference between the 2Y<sub>x</sub>Ce2Al and 1Y<sub>x</sub>Ce2Al grades is the significantly smaller grain-size of the (2Y<sub>x</sub>Ce)-TZP grades. As reported by Lange,<sup>21</sup> the grain-size of Y<sub>2</sub>O<sub>3</sub>-stabilised ZrO<sub>2</sub> decreases with increasing yttria content up to 2–3 mol%, and increases again with further yttria addition. Duh and Dai<sup>7</sup> found that a small addition of Y<sub>2</sub>O<sub>3</sub> in Ce-TZP resulted in an effective grain-size refinement. It is well established that the stability of the metastable tetragonal zirconia phase is affected by several microstructural and compositional parameters including grain-size and morphology, stabilizer type and content and matrix constraint. The grain-size and stabilizer content are believed to be the most important amongst these parameters. It should be clear, however, that the ZrO<sub>2</sub> ceramics with an yttria content below 1.4 mol% were reported to be fully monoclinic,<sup>21</sup> whereas the additional stabilisation by CeO<sub>2</sub> in this work resulted in TZP ceramics. Fig. 8 presents the average grain-size of all investigated material grades as a function of the sintering time at 1450 °C. The grain-size of all material grades increases linearly with the sintering time. The grain-size of the (1Y<sub>x</sub>Ce)-TZP and (2Y<sub>x</sub>Ce)-TZP materials clearly increases with increasing CeO<sub>2</sub> addition especially for the lower Y<sub>2</sub>O<sub>3</sub> content ceramics, as graphically illustrated for the 1Y4Ce2Al and 1Y8Ce2Al ceramics in Fig. 9.

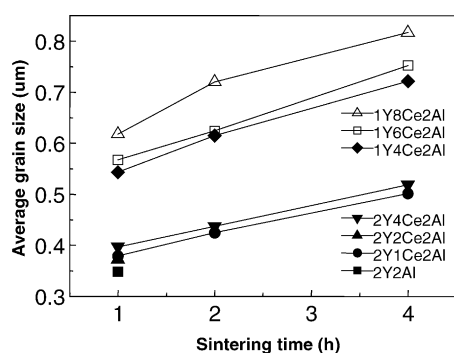


Fig. 8. Correlation of average grain-size and sintering time at 1450 °C.

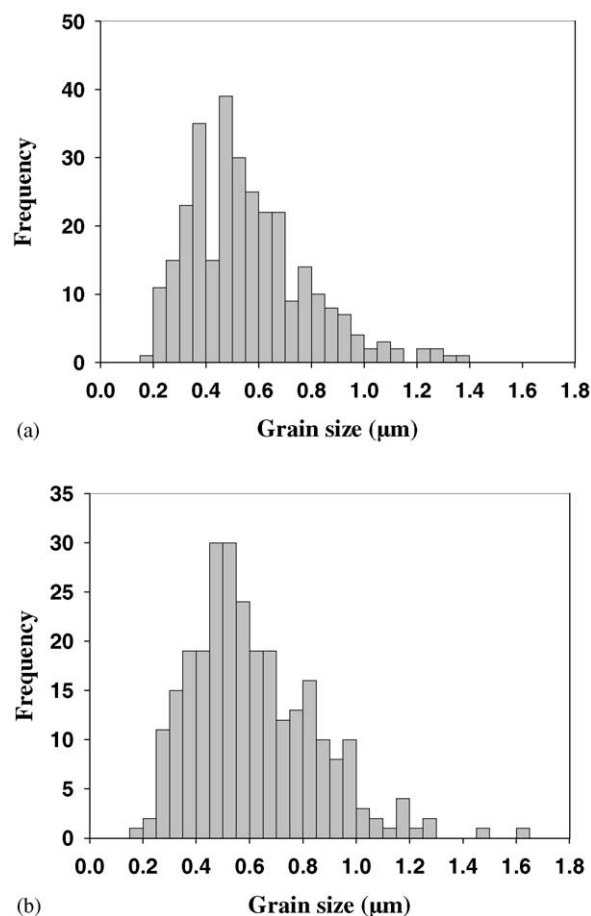


Fig. 9. Grain-size distribution of the 1Y4Ce2Al (a) and 1Y8Ce2Al (b) ceramics sintered for 1 h at 1450 °C.

Although no material grades without Al<sub>2</sub>O<sub>3</sub> addition were investigated, it can be deduced from literature that the addition of small amounts of Al<sub>2</sub>O<sub>3</sub> to a TZP matrix acts as a grain growth inhibitor and a sintering aid, enhancing densification during pressureless sintering and controlling the transformability and concomitant toughness of the material through tetragonal ZrO<sub>2</sub> grain-size control.<sup>10,11</sup>

To estimate the transformability of the t-ZrO<sub>2</sub> phase, the equilibrium temperature  $T_0$ , at which the chemical energy of the tetragonal and monoclinic phase are equal was calculated using Thermo-Calc.<sup>16</sup> The martensitic transformation temperature,  $M_s$ , of the samples sintered for 1 h at 1450 °C was calculated according to the formula reported by Zhang et al.<sup>19</sup> for the ZrO<sub>2</sub>–CeO<sub>2</sub>–Y<sub>2</sub>O<sub>3</sub> system. The calculated  $T_0$  and  $M_s$  of the selected compositions are summarized in Table 1. Since the martensitic transformation is enhanced in larger TZP grains, the largest measured grain-size intercept, listed in Table 1, was used in the calculation instead of the mean grain-size that was used in reference Zhang et al.<sup>19</sup> It is evident that the  $T_0$  decreases with increasing CeO<sub>2</sub> and Y<sub>2</sub>O<sub>3</sub> content. A higher  $T_0$  results in a higher  $M_s$  temperature, representing a higher transformability of the t-ZrO<sub>2</sub> phase and concomitant increasing fracture toughness. These

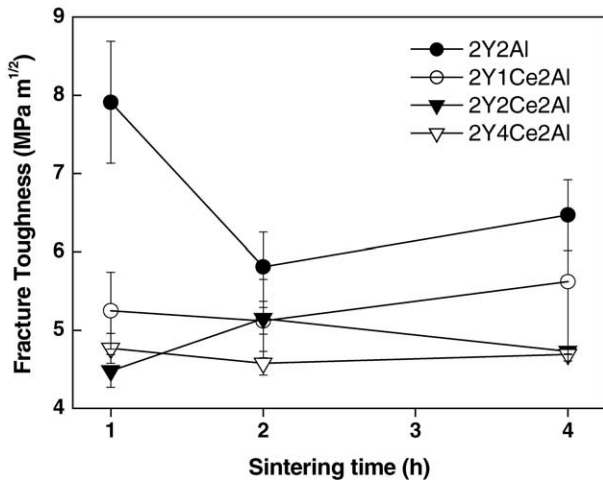


Fig. 10. Fracture toughness of the  $2Y_xCe_2Al$  as a function of the sintering time  $1450^\circ C$ .

calculations allow the explanation of the relative ranking of the experimental toughness measured for the  $(2Y_xCe)$ -TZP and  $(1Y_xCe)$ -TZP ceramics, sintered for 1 h at  $1450^\circ C$ .

The indentation toughness and hardness of the  $(2Y_xCe)$ -TZP materials is graphically presented as a function of the sintering time at  $1450^\circ C$  in Figs. 10 and 11. The highest toughness of  $8 MPa m^{1/2}$  was measured for the 2Y2Al ceramic after 1 h. The toughness, however, drastically decreased at longer sintering times due to spontaneous transformation of the  $t-ZrO_2$  phase as presented in Fig. 4. The calculated  $T_0$  and  $M_s$  of the 2Y2Al ceramic is higher than that of the other  $2Y_xCe_2Al$  ceramics, after 1 h of sintering at  $1450^\circ C$ , explaining the higher toughness. The  $M_s$  temperature of 2Y2Al, is close to room temperature, implying that the transformation toughness of this material grade should be high, as confirmed by the toughness measurements (see Fig. 10). The fracture toughness of the  $(2Y_xCe)$ -TZP grades with 1, 2 and 4 mol%  $CeO_2$  is comparable, around  $5 MPa m^{1/2}$  and hardly influenced by the sintering time up to

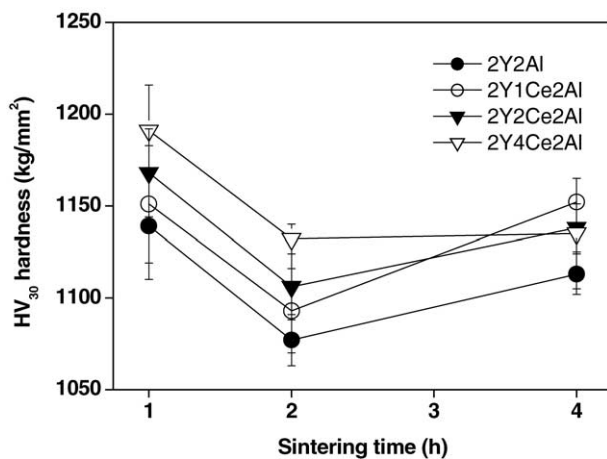


Fig. 11. Vickers hardness of the  $2Y_xCe_2Al$  ceramics as a function of the sintering time at  $1450^\circ C$ .

4 h. Despite the fact that the grain-size increases with increasing  $CeO_2$  addition (see Fig. 8), the hardness slightly increased with increasing  $CeO_2$  content when sintering for 1 or 2 h at  $1450^\circ C$  (see Fig. 11). The hardness trend amongst the samples sintered for 4 h as well as the evolution of the hardness as function of the sintering time is complex due to the interference of spontaneous transformation and the concomitant formation of microcracks.

The fracture toughness of the  $(1Y,8Ce)$ -TZP, plotted in Fig. 12, is comparable to that of the  $(2Y_xCe)$ -TZP grades with 1, 2 and 4 mol%  $CeO_2$ , whereas the hardness, graphically presented in Fig. 13, is lower due to the significantly larger grain-size (see Fig. 8). The fracture toughness drastically increases with decreasing  $CeO_2$  content in the  $(1Y_xCe)$ -TZP grades, whereas the hardness decreases. The addition of 2 mol%  $CeO_2$ , however, is not enough to stabilise the TZP material, as illustrated by the spontaneous transformation of the 1Y2Ce2Al ceramic. The increased hardness with increasing  $CeO_2$  addition is not so straightforward since the grain-size increases accordingly.

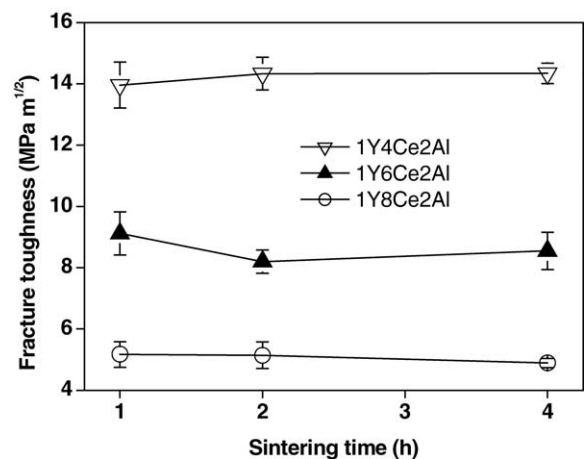


Fig. 12. Fracture toughness of the  $1Y_xCe_2Al$  as a function of the sintering time  $1450^\circ C$ .

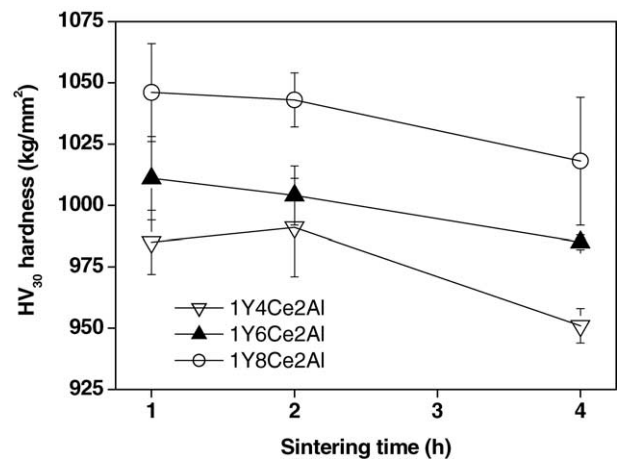


Fig. 13. Vickers hardness of the  $1Y_xCe_2Al$  ceramics as a function of the sintering time at  $1450^\circ C$ .

An excellent toughness of  $14 \text{ MPa m}^{1/2}$  was obtained for the 1Y4Ce2Al ceramic sintered for 1–4 h at  $1450^\circ\text{C}$ . An acceptable toughness of  $9 \text{ MPa m}^{1/2}$  was obtained for the 1Y6Ce2Al material, whereas the 1Y8Ce2Al grade has lower toughness of  $5 \text{ MPa m}^{1/2}$ . On the basis of thermodynamics, it is known that the transformability of these metastable materials increase with an increase in grain-size and a decrease in stabilizer content. The calculated  $T_0$  and  $M_s$  of the 1Y $_x$ Ce2Al grades are listed in Table 1. The  $T_0$  and  $M_s$  of the 1Y2Ce2Al grade is too high to retain all t-ZrO<sub>2</sub> at room temperature, resulting in spontaneous transformation as experimentally observed (see Fig. 5). The  $T_0$  and  $M_s$  decrease with increasing CeO<sub>2</sub> content, explaining the decreasing transformability and concomitant toughness of the 1Y $_x$ Ce2Al grades.

The hardness of the 1Y $_x$ Ce2Al ceramics decreases with increasing sintering temperature, which correlates with an increase in grain-size. For a given sintering time, the hardness, however, also increases with increasing CeO<sub>2</sub> content, what cannot be directly related to the difference in grain-size (Fig. 3) or density (Fig. 8).

## 5. Conclusions

Fully tetragonal (1Y,4–8Ce)-TZP and (2Y,1–4Ce)-TZP ceramics could be obtained when sintering mixed stabilizer-coated monoclinic ZrO<sub>2</sub> nanopowders with the addition of 2 wt.% Al<sub>2</sub>O<sub>3</sub> particles in air for 1–4 h at  $1450^\circ\text{C}$ .

The grain-size of (1Y, $_x$ Ce)-TZP and (2Y, $_x$ Ce)-TZP ceramics increases linearly with the CeO<sub>2</sub> content and sintering time. The grain-size of the 2 mol% Y<sub>2</sub>O<sub>3</sub> co-stabilised materials is significantly smaller than that of the 1 mol% Y<sub>2</sub>O<sub>3</sub> stabilised ceramics.

The indentation toughness of the 2Y $_x$ Ce2Al ceramics with  $x = 1–4$  mol% is comparable but lower than that of the 2 mol% Y<sub>2</sub>O<sub>3</sub> stabilised material, whereas the hardness is higher. The toughness of the 1Y $_x$ Ce2Al ceramics is strongly influenced by the CeO<sub>2</sub> content. A minimum CeO<sub>2</sub> content of 4 mol% was needed to avoid spontaneous transformation, resulting in an excellent toughness of  $14 \text{ MPa m}^{1/2}$ . A respectable toughness of  $8 \text{ MPa m}^{1/2}$  was obtained for the (1Y,6Ce)-TZP material whereas a modest toughness of  $5 \text{ MPa m}^{1/2}$  was measured for the (1Y,8Ce)-TZP ceramic. The toughness of the (2Y, $_x$ Ce)-TZP ceramics with 1–4 mol% CeO<sub>2</sub> was comparable to that of the (1Y,8Ce)-TZP material. The hardness of (2Y, $_x$ Ce)-TZP, however, is higher than that of (1Y, $_x$ Ce)-TZP due to the smaller grain-size of the former.

## Acknowledgements

This work is financially supported by the Research Fund K.U. Leuven: Flanders-China bilateral projects (BIL 99/10 and BIL 02/06), the Science and Technology Committee of Shanghai Municipality, and the State Key Lab of High Per-

formance Ceramics and Superfine Microstructure of Chinese Academy of Science.

## References

1. Anthony, G. E., Perspective on the development of high-toughness ceramics. *J. Am. Ceram. Soc.*, 1990, **73**, 187–206.
2. Hannink, R. H. J., Kelly, P. M. and Muddle, B. C., Transformation toughening in zirconia-containing ceramics. *J. Am. Ceram. Soc.*, 2000, **83**, 461–487.
3. Lin, J. D. and Duh, J. G., Crystallite size and microstrain of thermally aged low-ceria and low-yttria-doped zirconia. *J. Am. Ceram. Soc.*, 1998, **81**, 853–860.
4. Hirano, M. and Inada, H., Hydrothermal stability of yttria- and ceria-doped tetragonal zirconia–alumina composites. *J. Mater. Sci.*, 1991, **26**, 5047–5052.
5. Wang, J., Zheng, X. H. and Stevens, R., Fabrication and microstructure–mechanical property relationships in Ce-TZPs. *J. Mater. Sci.*, 1992, **27**, 5348–5356.
6. Tsukuma, K. and Shimada, M., Strength, fracture toughness and Vickers hardness of CeO<sub>2</sub>-stabilized tetragonal ZrO<sub>2</sub> polycrystals (Ce-TZP). *J. Mater. Sci.*, 1985, **20**, 1178–1184.
7. Duh, J. G. and Dai, H. T., Sintering, microstructure, hardness, and fracture toughness behaviour of Y<sub>2</sub>O<sub>3</sub>–CeO<sub>2</sub>–ZrO<sub>2</sub>. *J. Am. Ceram. Soc.*, 1988, **71**, 813–819.
8. Boutz, M. M. R., Winnubst, A. J. A. and Burggraaf, A. J., Yttria–ceria stabilised tetragonal zirconia polycrystals: sintering, grain growth and grain boundary segregation. *J. Eur. Ceram. Soc.*, 1994, **13**, 89–102.
9. Gritzner, G. and Steger, P., Y<sub>2</sub>O<sub>3</sub>–CeO<sub>2</sub>-doped ZrO<sub>2</sub> ceramics from coprecipitated oxalate precursors. *J. Eur. Ceram. Soc.*, 1993, **12**, 461–466.
10. Hirano, M. and Inada, H., Fracture toughness, strength and Vickers hardness of yttria–ceria doped tetragonal zirconia/alumina composites fabricated by hot isostatic pressing. *J. Mater. Sci.*, 1992, **27**, 3511–3518.
11. Vleugels, J., Yuan, Z. X. and Van Der Biest, O., Mechanical properties of Y<sub>2</sub>O<sub>3</sub>/Al<sub>2</sub>O<sub>3</sub>-coated Y-TZP ceramics. *J. Eur. Ceram. Soc.*, 2002, **22**, 873–881.
12. Yuan, Z. X., Vleugels, J. and Van Der Biest, O., Synthesis and characterisation of CeO<sub>2</sub>-coated ZrO<sub>2</sub> powder-based TZP. *Mater. Lett.*, 2000, **46**, 249–254.
13. Yuan, Z. X., Vleugels, J. and Van Der Biest, O., Preparation of Y<sub>2</sub>O<sub>3</sub>-coated ZrO<sub>2</sub> powder by suspension drying. *J. Mater. Sci. Lett.*, 2000, **19**, 359–361.
14. Li, L., Xu, Z. Y. and Ao, Q., Optimization of the phase diagram of CeO<sub>2</sub>–ZrO<sub>2</sub> system. *J. Mater. Sci. Technol.*, 1996, **12**, 159–160.
15. Li, L., Van Der Biest, O., Wang, P. L., Vleugels, J., Chen, W. W. and Huang, S. G., Estimation of the phase diagram for the ZrO<sub>2</sub>–Y<sub>2</sub>O<sub>3</sub>–CeO<sub>2</sub> system. *J. Eur. Ceram. Soc.*, 2001, **21**, 2903–2910.
16. Sundman, B., Jansson, B. and Andersson, J. O., The Thermo-Calc database system. *CALPHAD*, 1985, **9**, 153–190.
17. Mendelson, M. I., Average grain size in polycrystalline ceramics. *J. Am. Ceram. Soc.*, 1969, **52**, 443–446.
18. Anstis, G. R., Chantikul, P., Lawn, B. R. and Marshall, D. B., A critical evaluation of indentation techniques for measuring fracture toughness: I. Direct crack measurements. *J. Am. Ceram. Soc.*, 1981, **64**, 533–538.
19. Zhang, Y. L., Jin, X. J. and Hsu, T. Y., Thermodynamic calculation of  $M_s$  in ZrO<sub>2</sub>–CeO<sub>2</sub>–Y<sub>2</sub>O<sub>3</sub> system. *J. Eur. Ceram. Soc.*, 2003, **23**, 685–690.
20. Wang, J., Rainforth, M. and Stevens, R., The grain size dependence of the mechanical properties in TZP ceramics. *Br. Ceram. Trans. J.*, 1989, **88**, 1–6.
21. Lange, F. F., Transformation toughened ZrO<sub>2</sub>: correlations between grain size control and composition in the system ZrO<sub>2</sub>–Y<sub>2</sub>O<sub>3</sub>. *J. Am. Ceram. Soc.*, 1986, **69**, 240–242.